Applied Surface Science 270 (2013) 728–736

Contents lists available at SciVerse ScienceDirect

Applied Surface Science

journal homepage: www.elsevier.com/locate/apsusc

Influence of the hydroxylation of γ-Al_2O_3 surfaces on the stability and growth of Cu for Cu/γ-Al_2O_3 catalyst: A DFT study

Jingrui Li, Riguang Zhang, Baojun Wang*

Key Laboratory of Coal Science and Technology of Ministry of Education and Shanxi Province, Taiyuan University of Technology, Taiyuan 030024, Shanxi, China

ARTICLE INFO

Article history:
Received 12 December 2012
Received in revised form 20 January 2013
Accepted 20 January 2013
Available online 26 January 2013

Keyword:
Cu_n(n = 1–4) cluster
γ-Al_2O_3
Stability
Growth
Surface hydroxyl
Density functional theory

ABSTRACT

The interaction of Cu_n(n = 1–4) cluster with the dehydrated γ-Al_2O_3(110), hydrated γ-Al_2O_3(110) and dehydrated γ-Al_2O_3(100) surfaces has been systematically investigated to illustrate the influence of the hydroxylation of γ-Al_2O_3 surfaces on the stability and growth of Cu for Cu/γ-Al_2O_3 catalyst. Here, we present the main results obtained by the density functional theory together with slab model calculations. Our results show that the adsorption of Cu_n(n = 2–4) cluster on the γ-Al_2O_3(110) surface is more stable than that on the γ-Al_2O_3(100) surface, for the single Cu atom, the reverse becomes true. For the γ-Al_2O_3(110) surface, the adsorption of Cu_n(n = 2–4) cluster on the dehydrated surface is more stable than that on the hydrated surface due to the presence of the surface hydroxyls, however, the adsorption of the single Cu atom on the hydrated surface is more stable than that on the dehydrated surface due to the larger Cu–support interaction energy. On the other hand, compared to the γ-Al_2O_3(100) surface, the γ-Al_2O_3(110) surface is more favorable for the growth of Cu_n clusters, in which the presence of surface hydroxyls reduces the growth ability of Cu_n clusters.

1. Introduction

Heterogeneous catalysts play an important role in industrial catalytic processes [1]. Extensive experimental [2–5] and theoretical investigations [6,7] have been performed on the heterogeneous catalysts with transition metal deposited on various oxide surface, such as TiO_2, SiO_2, MgO [2,3], α-Al_2O_3[4], γ-Al_2O_3[6–8], α-Fe_2O_3[5], CeO_2[5] and ZrO_2[9]. Among them, γ-Al_2O_3 is one of the most common supports due to its high degree of porosity and surface area, thus favoring a good dispersion of the active phases [10]. Therefore, γ-Al_2O_3 supported metal catalysts have been widely used in many reactions[6,11–16], for example, Cu/γ-Al_2O_3 catalysts have been used for DME synthesis[17], methanol conversion[18], CO_2 hydrogenation to methanol[13,19]; Pd/γ-Al_2O_3 catalysts have been used for the oxidation of carbon monoxide, propene, propane, and methane[11]; Rh/γ-Al_2O_3 and Ir/γ-Al_2O_3 catalysts have been used for the hydrogenation reactions of ethene, propene, and toluene[20].

For heterogeneous catalysts, the aggregations of the metal active component on the support surface show good catalytic activities[14,21,22], as a result, supported metals are usually being used as small clusters or particles, which can be stably dispersed on the support surfaces[5,6,23], moreover, these small metal clusters or particles can often provide new properties due to the presence of low-coordination atoms and electron confinement effects[24], which is different from those of bulk metals. Meanwhile, previous studies [21,22,25–28] have shown that the catalytic properties of the metal clusters are markedly influenced by the metal sizes and the interactions of metal with support, for example, Prasad and co-workers [27,28] have found that the activity of Pd/Al_2O_3 catalyst is strongly dependent on Pd cluster shape and size for the hydrodechlorination of chlorobenzene, further, Meier et al. [29] also point out that the metal cluster size, the support material, or both, are critical to determining catalytic activity.

On the other hand, for heterogeneous catalysts, the nature of the support has an important influence on the stability and growth of metal particle, and further on the reactions taking place on this catalyst [30–32]. For γ-Al_2O_3-supported metal catalyst, the surface of the γ-Al_2O_3 support will inevitably be hydrated/hydroxylated under a realistic reaction condition; further, the nature of the surface will be modified [6,13,14,34–36]. This modification will lead to an influence on the active species–support interaction and further on the reactions taking place over the catalyst. For example, STM experiments for Rh particles supported on a thin hydroxylated alumina film revealed the change process for the growth and dispersion of metal particles [31,32]. Shi et al. [37] have studied the effect of surface hydroxyls on the nucleation and growth of γ-Al_2O_3 supported Rh cluster, suggesting that the growth of Rh preferentially occur on hydrated surfaces relative to dehydrated surfaces. Valero et al. [38] have studied the influence of metal coverage and its hydroxylation on the growth of Pd over the dehydrated

* Corresponding author at: No. 79 Yingze West Street, Taiyuan 030024, China. Tel.: +86 351 6018239; fax: +86 351 6041237.
E-mail addresses: wangbaojun@tyut.edu.cn, quantumtyut@126.com (B. Wang).

0169-4332/$ – see front matter © 2013 Elsevier B.V. All rights reserved.
http://dx.doi.org/10.1016/j.apsusc.2013.01.139

γ-Al_2O_3(100) and hydrated γ-Al_2O_3(110) surfaces, indicating that the growth at very low metal coverage on the hydrated surface is more favorable than that on the dehydrated surface, whereas, at a higher metal coverage, the reverse becomes true. Zhang et al. [39] have identified the hydroxylation effect of γ-Al_2O_3 support on the selectivity of CO_2 hydrogenation over Pd/γ-Al_2O_3 catalyst, indicating that varying the properties of γ-Al_2O_3 support can alter the selectivity of CO_2 hydrogenation, moreover, the presence and number of low-coordinated Pd particles is of great importance to improve the overall activity and selectivity of CO_2 hydrogenation.

Nowadays, Cu/γ-Al_2O_3 catalysts have been widely used for several catalytic applications [13,19,40–42], such as NO reduction [41], CO_2 hydrogenation to methanol[13,19], DME synthesis [17], methanol conversion [18]. However, up to now, to the best of our knowledge, few studies are carried out to investigate the influence of hydroxylation of γ-Al_2O_3 support on the stability and growth of Cu. Therefore, in this paper, we focus on the stability and growth of small Cu_n(n = 1–4) clusters on the γ-Al_2O_3 surfaces including the dehydrated (110), hydrated (110) and dehydrated (100) surfaces by using density functional theory method. We expect that our results are able to obtain the most stable adsorption configurations and favorable localization of Cu_n(n = 1–4) cluster on the γ-Al_2O_3 surfaces, metal–support interactions, and the influence of surface hydroxyls on the stability and growth of Cu.

2. Methods and models

2.1. Computational methods

All DFT calculations are performed using the Dmol^3 program available in Materials Studio 4.4 package [43,44]. The generalized gradient approximation (GGA) with Perdew-Burke- Ernzerhof (PBE) functional [45] is chosen together with the doubled numerical basis set plus polarization basis sets (DNP)[46]. The inner electrons of Cu and Al atoms are kept frozen and replace by an effective core potential (ECP)[47,48], and other atoms are treated with an all electron basis set. The k-point sampling scheme of Monkhorst-Pack grid of $2 \times 2 \times 1$ and Methfessel-Paxton smearing of 0.005 Hartree are used.

The binding energy, $E_{bind}(Cu_n)$, can be used to evaluate the stability of isolated Cu_n(n = 2–4) cluster per metallic atom, which is defined as follows [49]:

$$E_{bind}(Cu_n) = [n \times E(Cu) - E(Cu_n)]/n \quad (1)$$

where $E(Cu_n)$ and $E(Cu)$ are the total energies of isolated Cu_n cluster and a single Cu atom, respectively, n is the number of Cu atom in Cu_n clusters, herein, n = 2–4. The larger $E_{bind}(Cu_n)$ is, the isolated Cu_n(n = 2–4) cluster is more stable.

Similarly, the binding energy of Cu_n cluster supported on the γ-Al_2O_3 surface, $E_{bind}(Cu_n/\gamma\text{-}Al_2O_3)$, per metallic atom is given by the following equation [49]:

$$E_{bind}(Cu_n/\gamma\text{-}Al_2O_3) = [n \times E(Cu) + E(\gamma\text{-}Al_2O_3) - E(Cu_n/\gamma\text{-}Al_2O_3)]/n \quad (2)$$

where $E(Cu_n/\gamma\text{-}Al_2O_3)$ is the total energy of γ-Al_2O_3 slab with Cu_n cluster, $E(\gamma\text{-}Al_2O_3)$ is the total energy of bare γ-Al_2O_3 slab, herein, n = 2–4. $E_{bind}(Cu_n/\gamma\text{-}Al_2O_3)$ reflects the stability of Cu_n cluster supported on the γ-Al_2O_3 surface, the larger the value of $E_{bind}(Cu_n/\gamma\text{-}Al_2O_3)$ is, the Cu_n cluster supported on the γ-Al_2O_3 surface is more stable.

The adsorption energy of Cu_n(n = 1–4) cluster on the γ-Al_2O_3 surface, E_{ads}, is defined as follows:

$$E_{ads} = E(\gamma\text{-}Al_2O_3) + E(Cu_n) - E(Cu_n/\gamma\text{-}Al_2O_3) \quad (3)$$

Meanwhile, E_{ads} can be decomposed into deformation and interaction energy contributions. For the γ-Al_2O_3 surface, the surface deformation energy, $E_{def,surface}$, is calculated as the energy difference between the isolated γ-Al_2O_3 surface and the γ-Al_2O_3 surface in Cu_n/γ-Al_2O_3

$$E_{def,surface} = E(\gamma - Al_2O_3) - E(\gamma\text{-}Al_2O_3') \quad (4)$$

where $E(\gamma\text{-}Al_2O_3')$ is the total energy of γ-Al_2O_3 with the deformed geometry obtained after Cu_n adsorption. With the definition, the smaller the $E_{def,surface}$ is, the stronger the surface deformation is. For the Cu_n cluster, the cluster deformation energy is calculated as

$$E_{def,Cun} = E(Cu_n) - E(Cu_n') \quad (5)$$

where $E(Cu_n')$ is the total energy of Cu_n cluster supported on the γ-Al_2O_3 surface. Finally, the cluster–support interaction energy, E_{int}, is defined as follows:

$$E_{int} = E(Cu_n') + E(\gamma - Al_2O_3') - E(Cu_n/\gamma\text{-}Al_2O_3) \quad (6)$$

From Eqs. (3)–(6), it can be seen that $E_{ads} = E_{def,Cun} + E_{def,surface} + E_{int}$.

2.2. Computational models

The γ-Al_2O_3 structural models based on the defective spinel model [50,51] and non-spinel model [33] have been proposed. In this study, we employ the non-spinel model based on the fact that its (100) surface exposes the penta-Al sites that is observed experimentally [52,53]. The non-spinel γ-Al_2O_3 model has been used to construct surfaces in the previous studies [54–56], thus, we employ non-spinel-γ-Al_2O_3 as in the previous studies to model the γ-Al_2O_3 surface in this work. Meanwhile, the (110) and (100) surfaces are selected on the basis of the fact that the (110) surface is estimated to comprise 83% of the total surface area of γ-Al_2O_3 [33,57,58], and a completely dehydrated γ-Al_2O_3 surface is probably best represented by the (100) surface of the non-spinel γ-Al_2O_3 model[32].

For the γ-Al_2O_3(110) surface, we have considered the dehydrated (110) surface and hydrated (110) surface. The (110) surface is modeled by a supercell with a dimension of 8.41 Å × 8.07 Å × 19.17 Å. Twelve Al_2O_3 molecular units in the slab are distributed in six layers. The vacuum region separating the slabs in the direction perpendicular to the surface direction is set to 12 Å. In all calculations, the bottom two layers are frozen in their bulk positions, whereas the remaining four layers together with the adsorbed Cu_n(n = 1–4) cluster and/or hydroxyls are allowed to relax. On the other hand, the supercell for (100) surface includes ten atomic layers with a vacuum region of 12 Å, resulting in a supercell size of 11.17 Å × 8.41 Å × 20.44 Å. In this case, the adsorbed Cu_n(n = 1–4) cluster together with the top six layers are allowed to relax. The dehydrated and hydrated γ-Al_2O_3(110) surface, dehydrated γ-Al_2O_3(100) are shown in Fig. 1.

3. Results and discussion

3.1. Isolated Cu_n clusters

In this section, we first investigate the geometries of isolated Cu_n clusters, which are essential to understand the growth of Cu_n cluster on the γ-Al_2O_3 surfaces. The geometries and structure parameters of Cu_n(n = 2–4) cluster are obtained. One-dimensional (1D), two-dimensional (2D), and three-dimensional (3D) structures of Cu_n clusters are considered, and only the most stable configurations are summarized in Table 1. For Cu_4 cluster, the isolated 3D tetrahedral configuration is less stable than the isolated 2D planar one. However, upon binding on γ-Al_2O_3(100) and (110) surfaces, the tetrahedral configuration shows a stronger interaction

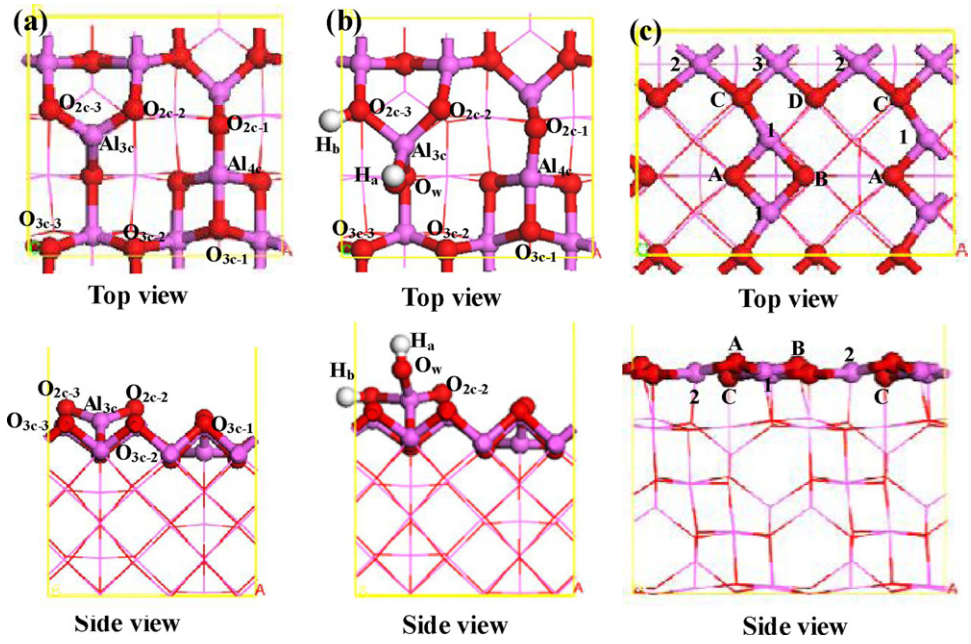

Fig. 1. The top and side views of (a) the dehydrated γ-Al_2O_3(110) surface, (b) the hydrated γ-Al_2O_3(110) surface, and (c) the dehydrated γ-Al_2O_3(100) surface. Pink, red and white balls stand for Al, O and H atoms, respectively.

Table 1
The geometry, the average Cu–Cu bond lengths, the binding energy of isolated Cu_n(n = 2–4) cluster, E_{bind} (Cu_n).

n	Geometry	$\bar{d}(Cu–Cu)$ (Å)	$E_{bind}(Cu_n)$ (kJ mol^{-1})
2	$D_{\infty h}$	2.277	97.0
3	D_{3h}	2.415	104.3
4	T_d	2.472	113.6

than planar configurations. Further, on the basis of the facts that the tetrahedral configuration is the smallest unit, which can provides a 3D structure to probe both metal–metal and metal–support interactions [59,60]. Therefore, we focus our attentions on the tetrahedral configuration in the present study.

From Table 1, we can see that the Cu–Cu bond lengths increase with the cluster size increasing, however, they are shorter than those found in bulk structure (d(Cu–Cu) = 2.556 Å), and cannot reach bulk value. The geometries of Cu_2, Cu_3 and Cu_4 clusters are $D_{\infty h}$, D_{3h}, and T_d point groups, respectively. As expected, with the increase of atomic coordination in cluster, the values of $E_{bind}(Cu_n)$ increase.

3.2. Adsorption of Cu_n cluster on different γ-Al_2O_3 surfaces

3.2.1. Dehydrated γ-Al_2O_3(110) surface

The side and top views of the dehydrated γ-Al_2O_3(110) surface are presented in Fig. 1(a). On this surface, the three-fold-coordinated aluminum (Al_{3c}), four-fold-coordinated aluminum (Al_{4c}), six-fold-coordinated aluminum (Al_{6c}), two-fold-coordinated oxygen ($O_{2c\text{-}1}$, $O_{2c\text{-}2}$ and $O_{2c\text{-}3}$) and three-fold-coordinated oxygen ($O_{3c\text{-}1}$, $O_{3c\text{-}2}$ and $O_{3c\text{-}3}$) atoms are exposed, among which Al_{3c}, Al_{4c}, $O_{2c\text{-}1}$, $O_{2c\text{-}2}$ and $O_{2c\text{-}3}$ are coordinately unsaturated.

A number of sites on the dehydrated γ-Al_2O_3(110) surface have been explored for Cu_n(n = 1–4) cluster adsorption, and the most stable adsorption configurations are presented in Fig. 2. The corresponding key parameters for these clusters are listed in Table 2.

As shown in Fig. 2(a), a single Cu atom on the dehydrated (110) surface binds to O_{2c} and Al_{4c} sites, the corresponding adsorption energy is 144.2 kJ mol^{-1}. The adsorption of the single Cu atom can introduce a surface deformation with the surface deformation energy of −59.8 kJ mol^{-1}. The Cu_1–support interaction energy is 204.0 kJ mol^{-1}, which mainly contribute to the adsorption energy. The bond lengths of Cu–$O_{2c\text{-}1}$, Cu–$O_{2c\text{-}2}$ and Cu–Al_{4c} are 1.973, 1.998 and 2.521 Å, respectively. The most stable adsorption configuration of the single Cu atom adsorbed on the dehydrated (110) surface is in good agreement with Rh atom adsorption [8].

For Cu_2 cluster, the most stable adsorption configuration is shown in Fig. 2(b), which is also similar to that of Rh[8]. The distance between Cu1 and Cu2 atoms is 2.313 Å, which is longer than that in the isolated Cu_2 cluster (2.277 Å). The bond lengths of Cu1–$O_{2c\text{-}1}$, Cu1–$O_{2c\text{-}2}$, Cu1–Al_{3c} and Cu1–Al_{4c} are 2.027, 2.004, 2.637 and 2.462 Å, respectively. The bond lengths of Cu2–Al_{3c} and Cu2–$O_{3c\text{-}2}$ are 2.530 and 2.047 Å, respectively. The adsorption energy of Cu_2 cluster is 264.9 kJ mol^{-1}, which is larger than that for the single Cu atom due to its increase of the Cu–support interaction energy to 385.5 kJ mol^{-1} from 204.0 kJ mol^{-1} for the single Cu atom, suggesting that the Cu_2–support interaction energy makes a major

Table 2
The adsorption energy, E_{ads}, interaction energy, E_{int}, Cu_n deformation energy, $E_{def,Cun}$, surface deformation energy, $E_{def,surface}$, the binding energy of Cu_n clusters supported on γ-Al_2O_3 surfaces per metallic atom, $E_{bind}(Cu_n/\gamma\text{-}Al_2O_3)$, and the average Cu–Cu bond lengths $\bar{d}(Cu–Cu)$ of Cu_n cluster adsorbed on dehydrated γ-Al_2O_3(110) surface.

n	E_{ads} (kJ mol^{-1})	E_{int} (kJ mol^{-1})	$E_{def,Cun}$ (kJ mol^{-1})	$E_{def,surface}$ (kJ mol^{-1})	$\bar{d}(Cu–Cu)$ (Å)
1	144.2	204.0	–	−59.8	–
2	264.9	385.5	−0.7	−119.9	2.313
3	347.1	461.3	−1.3	−112.9	2.424
4	412.1	568.5	−4.4	−152.0	2.514

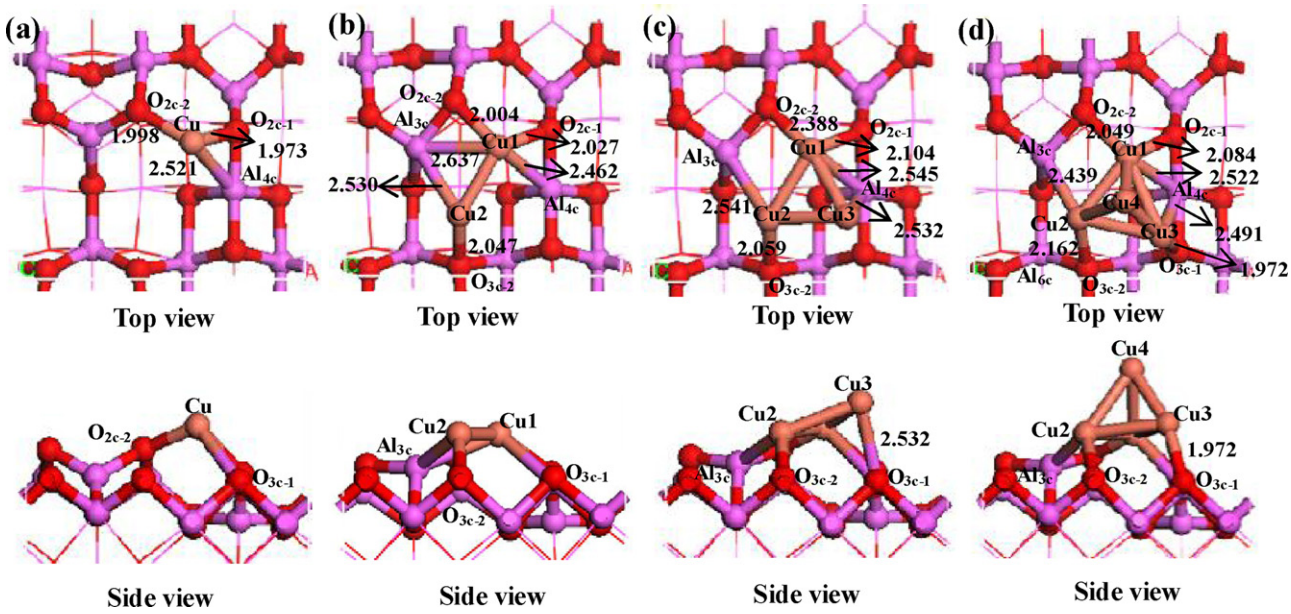

Fig. 2. The most stable adsorption configurations of Cu_n(n = 1–4) clusters on the dehydrated γ-Al_2O_3(110) surface for (a) Cu_1, (b) Cu_2, (c) Cu_3 and (d) Cu_4. Bond lengths are in Å. Orange balls stand for Cu atoms, and others are the same as in Fig. 1.

contribution to the adsorption energy. The surface deformation energy is −119.9 kJ mol^{-1}, and is lower than that for the single Cu atom (−59.8 kJ mol^{-1}), indicating that the adsorption of Cu_2 cluster introduces much stronger surface deformation than that for the adsorption of the single Cu atom. The Cu_2 cluster deformation energy is −0.7 kJ mol^{-1}, and makes a little contribution to the adsorption energy.

For Cu_3 cluster, as presented in Fig. 2(c), the most stable adsorption configuration is the plane of Cu_3 triangular cluster lying aslant on the surface, and forming two Cu1–O_{2c} bonds (2.104 and 2.388 Å), Cu–O_{3c} bond (2.059 Å), Cu–Al_{3c} bond (2.541 Å), and two Cu–Al_{4c} bonds (2.545 and 2.532 Å). The adsorption energy of Cu_3 cluster is 347.1 kJ mol^{-1}, which is larger than that for Cu_2 cluster (264.9 kJ mol^{-1}). The Cu_3–support interaction strongly increases to 461.3 kJ mol^{-1} from 385.5 kJ mol^{-1} for Cu_2 cluster. The surface deformation energy is −112.9 kJ mol^{-1}, which is close to that for Cu_2 cluster (−119.9 kJ mol^{-1}). The small difference of surface deformation energy between Cu_2 and Cu_3 clusters indicates that the increase of Cu_3–support interaction energy is a major contribution to the increase of the adsorption energy. The Cu_3 cluster deformation energy (−1.3 kJ mol^{-1}) contributes little to the adsorption energy.

For Cu_4 cluster, as shown in Fig. 2(d), the most stable adsorption configuration of Cu_4 cluster supported on dehydrated γ-Al_2O_3(110) surface is similar to that obtained by Zhang et al. [19]. In this configuration, three Cu atoms (Cu1, Cu2 and Cu3) interact with the surface directly, forming two Cu1–O_{2c} bonds (2.084 and 2.049 Å), two Cu–O_{3c} bonds (1.972 and 2.162 Å), Cu–Al_{3c} bond (2.439 Å), and two Cu–Al_{4c} bonds (2.522 and 2.491 Å), Cu4 atom is located at the top vertex away from the support surface. The adsorption energy of Cu_4 cluster is 412.1 kJ mol^{-1} and in good agreement with the previous result (405.6 kJ mol^{-1}) [19]. The Cu_4–support interaction strongly increases to 568.5 kJ mol^{-1} from 461.3 kJ mol^{-1} for Cu_3 cluster, which makes a major contribution to the increase of the adsorption energy. The surface deformation energy is −152.0 kJ mol^{-1}, and is smaller than that for Cu_3 cluster (−112.9 kJ mol^{-1}), suggesting that the adsorption of Cu_4 cluster introduces much stronger surface deformation than that for the adsorption of Cu_3 cluster. The Cu_4 cluster deformation energy is −4.4 kJ mol^{-1}, and gives a negligible contribution to the adsorption energy.

On the basis of above results, we can see that on dehydrated γ-Al_2O_3(110) surface, there is a strong correlation among the adsorption energy of Cu_n clusters, surface deformation, Cu_n cluster deformation and Cu–support interaction energies. Cu_n cluster deformation has little impact on the final measured adsorption energy, and makes a little contribution to the adsorption energy. As listed in Table 2, with the increase of Cu_n clusters size, both the adsorption energy of Cu_n cluster and the Cu–support interaction energy increase, moreover, the increase of the Cu–support interaction energy mainly contribute to the increase of the adsorption energy. For all supported clusters from Cu_2 to Cu_4, the average Cu–Cu bond length is larger than that for the corresponding isolated cluster.

3.2.2. *Adsorption on the hydrated γ-Al_2O_3(110) surface*

The schematic views of the hydrated γ-Al_2O_3(110) surface are presented in Fig. 1(b). The key feature of the surface is that a hydroxyl group (O_wH_a) binds to a surface Al_{3c} site, whereas a proton (H_b) binds to a surface $O_{2c\text{-}3}$ site, forming two surface OH groups in one unit cell.

A number of sites on the hydrated γ-Al_2O_3(110) surface have also been explored for Cu_n clusters adsorption. Only the most stable adsorption configurations are shown in Fig. 3, and the corresponding key parameters are listed in Table 3.

For a single Cu atom, as shown in Fig. 3(a), the single Cu atom prefers to bind to the surface hydroxyl and $O_{3c\text{-}2}$ site, which is in good agreement with the previous results [37,38]. The bond lengths of Cu–O_w and Cu–$O_{3c\text{-}2}$ are 1.879 and 1.875 Å, respectively. The adsorption energy is 168.0 kJ mol^{-1}, which is larger than that on the dehydrated γ-Al_2O_3(110) (144.2 kJ mol^{-1}). The adsorption of the single Cu atom leads to a strong surface deformation with the surface deformation energy is −123.1 kJ mol^{-1}. The Cu_1–support interaction energy (291.1 kJ mol^{-1}) is larger than that for the single Cu atom on the dehydrated γ-Al_2O_3(110) (204.0 kJ mol^{-1}), which makes a major contribution to the adsorption energy.

For Cu_2 cluster, as shown in Fig. 3(b), one Cu atom binds to the surface $O_{2c\text{-}2}$ and Al_{4c} sites, and the other Cu atom binds to the surface $O_{3c\text{-}2}$ and Al_{4c} sites. The bond lengths of Cu1–$O_{2c\text{-}2}$, Cu1–Al_{4c}, Cu2–$O_{3c\text{-}2}$ and Cu2–Al_{4c} are 2.098, 2.403, 2.137 and 2.667 Å, respectively. The Cu_2 cluster is nearly parallel to the

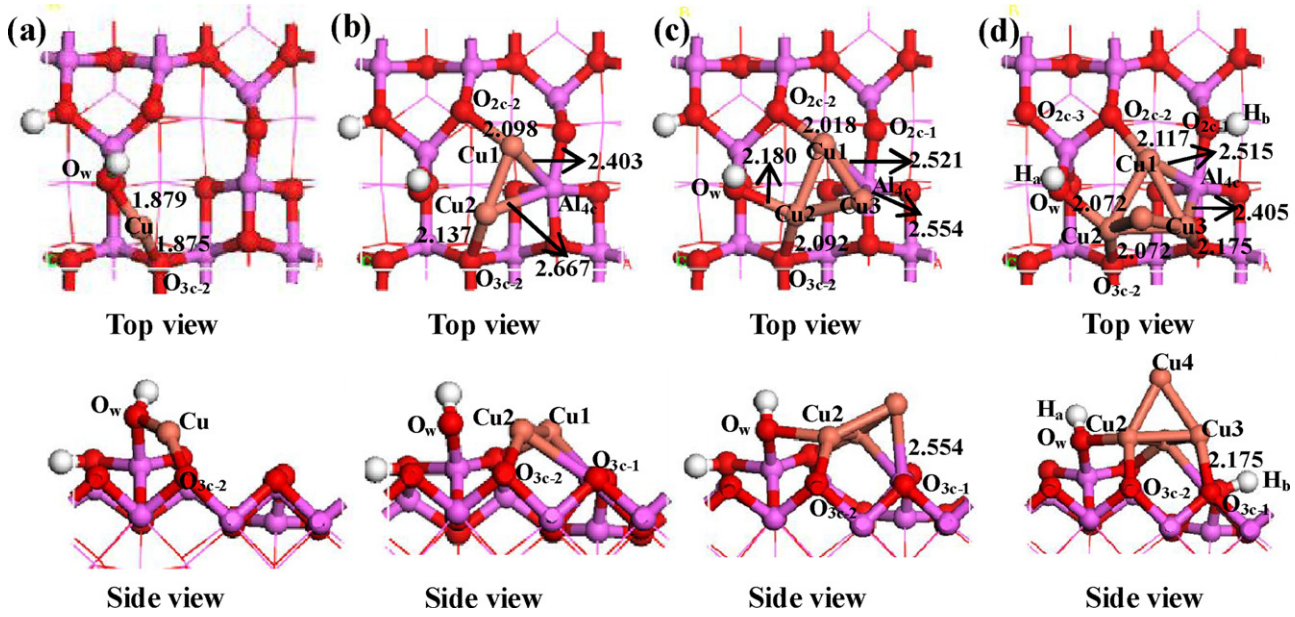

Fig. 3. The adsorption of Cu_n(n = 1–4) clusters on the hydrated γ-Al_2O_3(110) surface for (a) Cu_1, (b) Cu_2, (c) Cu_3 and (d) Cu_4 clusters. Bond lengths are in Å. See Figs. 1 and 2 for color coding.

surface plane. The bond length of Cu1–Cu2 (2.318 Å) is larger than that in the isolated Cu_2 cluster (2.277 Å). The adsorption energy of Cu_2 cluster (221.7 kJ mol^{-1}) and Cu_2–support interaction energy (309.4 kJ mol^{-1}) are smaller than the corresponding energies on the dehydrated γ-Al_2O_3(110) surface (264.9 and 385.5 kJ mol^{-1}) due to the presence of the surface hydroxyls. The decrease of Cu_2–support interaction energy is responsible for the decrease of the adsorption energy. The Cu_2 cluster deformation energy (−0.6 kJ mol^{-1}) has a negligible contribution to the adsorption energy. The surface deformation energy (−87.1 kJ mol^{-1}) is larger than that on the dehydrated γ-Al_2O_3(110) surface (−119.9 kJ mol^{-1}), suggesting that the presence of the surface hydroxyls can increase the stability of the γ-Al_2O_3(110) surface.

For Cu_3 cluster, as shown in Fig. 3(c), the most stable adsorption configuration is similar to that on the dehydrated (110) surface, and the average bond length of Cu–Cu (2.406 Å) is smaller than that on the dehydrated (110) surface (2.424 Å). The bond lengths of Cu1–$O_{2c\text{-}2}$, Cu2–$O_{3c\text{-}2}$ and Cu2–O_w bonds are 2.018, 2.092 and 2.180 Å, respectively. The bond lengths of two Cu–Al_{4c} bonds are 2.521 and 2.554 Å, respectively. Owing to the presence of the surface hydroxyls, the adsorption energy of Cu_3 cluster (321.4 kJ mol^{-1}) and Cu_3–support interaction energy (428.2 kJ mol^{-1}) decrease relative to the corresponding energies on the dehydrated γ-Al_2O_3(110) surface (347.1 and 461.3 kJ mol^{-1}). The surface deformation energy (−106.5 kJ mol^{-1}) is close to that for the dehydrated γ-Al_2O_3(110) surface (−112.9 kJ mol^{-1}), this small difference indicates that the decrease of Cu_3–support interaction energy is a major contribution to the decrease of the adsorption energy. The Cu_3 cluster deformation energy (−0.3 kJ mol^{-1}) has few contributions to the adsorption energy.

For Cu_4 cluster, as shown in Fig. 3(d), the cluster interacts with the surface through three Cu atoms (Cu1, Cu2 and Cu3), and forming Cu1–$O_{2c\text{-}2}$ bond (2.117 Å), Cu2–$O_{3c\text{-}2}$ bond (2.072 Å), Cu2–O_w bond (2.072 Å), Cu3–$O_{3c\text{-}1}$ bond (2.175 Å) and two Cu–Al_{4c} bonds (2.515 and 2.405 Å). The adsorption of Cu_4 cluster leads to the migration of H_b atom from $O_{2c\text{-}3}$ to $O_{2c\text{-}1}$ site, and a Cu–Cu bond cleavage in the isolated Cu_4 cluster. The adsorption energy and Cu_4–support interaction energy are 367.7 and 502.1 kJ mol^{-1}, respectively. Due to the presence of the surface hydroxyls, both the adsorption energy of Cu_4 cluster and the Cu_4–support interaction energy are smaller than the corresponding energies (412.1 and 568.5 kJ mol^{-1}) for the dehydrated γ-Al_2O_3(110) surface. Moreover, the decrease of Cu_4–support interaction energy mainly leads to the decrease of the adsorption energy. The increase of the surface deformation energy from −152.0 kJ mol^{-1} for the dehydrated γ-Al_2O_3(110) surface to −133.5 kJ mol^{-1} for the hydrated γ-Al_2O_3(110) surface still indicate that the presence of the surface hydroxyls is in favor of the stability of the surface. Similarly, the Cu_4 cluster deformation energy (−0.9 kJ mol^{-1}) makes a negligible contribution to the adsorption energy.

In addition, Valero et al. [38] have investigated the most stable configurations for Pd_4 clusters supported on the hydrated γ-Al_2O_3(110) surface. Yin et al. [13] and Pan et al. [14] have studied the adsorption of Co_4 [13] and Ni_4 [14] clusters on the hydrated γ-Al_2O_3(110) surface. These results indicate that the stable adsorption configurations of Pd_4, Co_4 and Ni_4 clusters are different from that of Cu_4 cluster. Therefore, we can conclude that different metals adsorbed on the same γ-Al_2O_3 surface may have the different adsorption sites and the stable configurations.

From above calculated results, we can see that on the hydrated γ-Al_2O_3(110) surface, there is still a strong correlation among the

Table 3
The adsorption energy, E_{ads}, interaction energy, E_{int}, Cu_n deformation energy, $E_{def,Cun}$, surface deformation energy, $E_{def,surface}$, and average Cu–Cu bond lengths $\bar{d}$(Cu–Cu) of Cu_n cluster supported on the hydrated γ-Al_2O_3(110) surface.

n	E_{ads} (kJ mol^{-1})	E_{int} (kJ mol^{-1})	$E_{def,Cun}$ (kJ·mol^{-1})	$E_{def,surface}$ (kJ mol^{-1})	$\bar{d}$(Cu–Cu) (Å)
1	168.0	291.1	–	-123.1	–
2	221.7	309.4	−0.6	−87.1	2.318
3	321.4	428.2	−0.3	−106.5	2.406
4	367.7	502.1	−0.9	−133.5	2.444

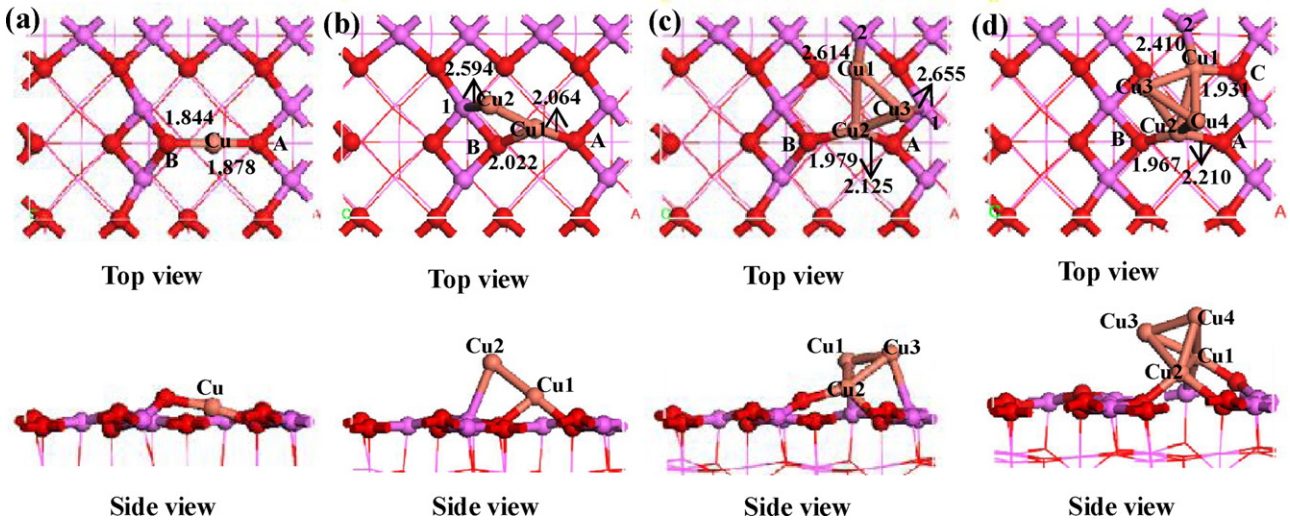

Fig. 4. The adsorption of Cu_n(n = 1–4) cluster on the dehydrated γ-Al_2O_3(100) surface for (a) Cu_1, (b) Cu_2, (c) Cu_3 and (d) Cu_4 clusters. Bond lengths are in Å. See Figs 1 and 2 for color coding.

adsorption energy of Cu_n clusters, surface deformation, Cu_n cluster deformation and Cu–support interaction energies, in which the Cu_n cluster deformation has relatively little influence on the adsorption energy. Compared to the dehydrated (110) surface, both the adsorption energies of Cu_n clusters and Cu–support interaction energy for the hydrated γ-Al_2O_3(110) surface follow the same trend, i.e., $Cu_1 < Cu_2 < Cu_3 < Cu_4$, however, for Cu_n(n = 2–4) cluster, due to the presence of the surface hydroxyls, they are smaller than the corresponding energies on the dehydrated (110) surface. For the single Cu atom, because of the larger Cu_1–support interaction and the stronger surface deformation, the adsorption energy on the hydrated (110) surface is larger than that on the dehydrated (110) surface. The Cu–support interaction energy gives a considerable contribution to the adsorption energy of Cu_n(n = 1–4) clusters. For the Cu_n(n = 2–4) clusters, the surface deformation energy of the hydrated (110) surface is higher than the corresponding energy of the dehydrated (110) surface, suggesting that the presence of the surface hydroxyls is favorable for the stability of the (110) surface. Meanwhile, the adsorption of Rh on the dehydrated and hydrated γ-Al_2O_3(100) surfaces [37] also indicate that the presence of the surface hydroxyls is favorable for the stability of the γ-Al_2O_3 surface.

3.2.3. Dehydrated γ-Al_2O_3(100) surface

For the adsorption of Cu_n(n = 1–4) cluster on the dehydrated γ-Al_2O_3(100) surface, we have considered a large number of sites, such as seven top sites, denoted O(A), O(B), O(C), O(D), Al(1), Al(2) and Al(3), fifteen bridge sites (O(A)–O(C), O(C)–O(D), two O(A)–O(B), O(B)–O(D), Al(1)–O(A), Al(1)–O(B), Al(1)–O(C), Al(1)–O(D), Al(2)–O(C), Al(2)–O(D), Al(3)–O(C), Al(3)–O(D), two Al(2)–Al(3)), and one hollow site consisting of four O atoms, and explored a large number of adsorption configurations. The most stable adsorption configurations are shown in Fig. 4, and the corresponding key parameters are listed in Table 4.

As shown in Fig. 4(a), the most favorable adsorption site of a single Cu atom on the dehydrated γ-Al_2O_3(100) surface is found to be an O(A)–O(B) bridge site. The bond lengths of Cu–O(A) and Cu–O(B) are 1.878 and 1.844 Å, respectively. The adsorption energy of single Cu atom is 177.3 kJ mol^{-1}, which is larger than that on the γ-Al_2O_3(110) surfaces. The Cu_1–support interaction energy is 246.4 kJ mol^{-1}, and makes a major contribution to the adsorption energy. The surface deformation energy is −69.1 kJ mol^{-1}. The adsorbate-induced surface deformation on γ-Al_2O_3(100) surface has also been observed for Rh [37] and Pd [38].

For Cu_2 cluster, the most stable adsorption configuration is shown in Fig. 4(b). The Cu_2 cluster is adsorbed aslant on the surface with Cu_2 atom locating at Al(1) site, and Cu_1 atom locating at the O(A)–O(B) bridge site. The bond length of Cu1–Cu2 (2.411 Å) is longer than that in the isolated Cu_2 cluster (2.277 Å). The bond lengths of Cu1–O(A), Cu1–O(B) and Cu2–Al(1) are 2.064, 2.022 and 2.594 Å, respectively. Both the adsorption energy of Cu_2 cluster (156.3 kJ mol^{-1}) and Cu_2–support interaction energy (230.8 kJ mol^{-1}) are smaller than the corresponding energies for the single Cu atom (177.3 kJ·mol^{-1} and 246.4 kJ mol^{-1}). The surface deformation energy for Cu_2 cluster (−68.8 kJ mol^{-1}) and the single Cu atom (−69.1 kJ mol^{-1}) are nearly equal, indicating that the decrease of the adsorption energy for Cu_2 cluster is mainly due to the decrease of Cu_2–support interaction energy. In addition, the deformation energy of Cu_2 cluster is also small (−5.7 kJ mol^{-1}) and contributes little to the adsorption energy.

For Cu_3 cluster, the most stable adsorption configuration is presented in Fig. 4(c), the plane of Cu_3 cluster lies aslant on the surface forming Cu1–Al(2) (2.614 Å), Cu2–O(A) (2.125 Å), Cu2–O(B) (1.979 Å) and Cu3–Al(1) bonds (2.655 Å). The adsorption energy of Cu_3 cluster is 238.5 kJ mol^{-1}, which is larger than that for Cu_2 cluster (156.3 kJ mol^{-1}). Meanwhile, compared to the Cu_2 cluster, the adsorption of Cu_3 cluster is accompanied by a relatively strong surface deformation with the surface deformation energy

Table 4
The adsorption energy, E_{ads}, interaction energy, E_{int}, Cu_n deformation energy, $E_{def,Cun}$, surface deformation energy, $E_{def,surface}$, and average Cu–Cu bond distances $\bar{d}$(Cu–Cu) of Cu_n cluster adsorbed on the dehydrated γ-Al_2O_3(100) surface.

n	E_{ads} (kJ mol^{-1})	E_{int} (kJ mol^{-1})	$E_{def,Cun}$ (kJ mol^{-1})	$E_{def,surface}$ (kJ·mol^{-1})	$\bar{d}$(Cu–Cu) (Å)
1	177.3	246.4	–	−69.1	–
2	156.3	230.8	−5.7	−68.8	2.411
3	238.5	334.5	−4.0	−92.0	2.494
4	291.0	499.4	−3.4	−205.0	2.518

is −92.0 kJ mol^{-1}. The Cu_3–support interaction strongly increases to 334.5 kJ mol^{-1} from 230.8 kJ mol^{-1} for Cu_2 cluster, which mainly contributes to the increase of the adsorption energy for Cu_3 cluster, whereas, the Cu_3 cluster deformation has a smaller contribution to the adsorption energy.

For Cu_4 cluster, the most stable configuration is shown in Fig. 4(d), two Cu atoms bind with the surface through the Cu1–Al(2) (2.410 Å), Cu1–O(C) (1.931 Å), Cu2–O(A) (2.210 Å) and Cu2–O(B) (1.967 Å) bonds, and the adsorption energy is 291.0 kJ·mol^{-1}, which is larger than those for other Cu_n cluster. The adsorption of Cu_4 cluster introduces a stronger surface deformation (−205.0 kJ mol^{-1}) compared to those for other Cu_n clusters, however, the cluster deformation energy (−3.4 kJ mol^{-1}) is also negligible. The Cu_4–support interaction energy (499.4 kJ mol^{-1}) is also larger than those for other Cu_n clusters, which is the main reason of the larger adsorption energy of Cu_4 cluster.

The most adsorption configurations of Rh_n [37] and Pd_n [38] (n = 1–5) on γ-Al_2O_3(100) surface have been obtained by the previous studies, which are different from the most stable adsorption configurations of Cu_n. Therefore, based on the above fact, we can think that there are different stable adsorption configurations for different metals on the γ-Al_2O_3(100) surface. Our results demonstrate that the Cu_n cluster deformation plays negligible role in the final measured adsorption energy. As listed in Table 4, with the increase of Cu_n(n = 2–4) cluster size, both the adsorption energy of Cu_n cluster and Cu–support interaction increase, moreover, the increase of Cu–support interaction give a dominant contribution to the increase of the adsorption energy. For all supported clusters from Cu_2 to Cu_4, the average Cu–Cu bond length (2.411, 2.494, 2.518 Å) is larger than that for the corresponding isolated cluster (2.277, 2.415 and 2.472 Å).

3.2.4. Stability summary

From Tables 2–4, we can see that, for the Cu_n(n = 2–4) cluster, the adsorption energy on the γ-Al_2O_3(110) surface is larger than that on the γ-Al_2O_3(100) surface, indicating that the adsorption of Cu_n(n = 2–4) cluster on the γ-Al_2O_3(110) surface is more stable than that on the γ-Al_2O_3(100) surface, however, for the single Cu atom, the reverse becomes true.

For γ-Al_2O_3(110), both the adsorption energy of Cu_n cluster and Cu–support interaction energy on the dehydrated and hydrated surfaces follow the same trend: Cu_1<Cu_2<Cu_3<Cu_4. Compared to the dehydrated surface, the larger adsorption energy of the single Cu atom on the hydrated surface is due to the stronger deformation of surface. For the Cu_n(n = 2–4) cluster, both the adsorption energy and the Cu–support interaction energy for the dehydrated surface are larger than the corresponding energies for the hydrated surface, suggesting that the surface hydroxyls have a negative influence on the adsorption of Cu_n(n = 2–4) cluster, and lower the interaction between Cu_n cluster and γ-Al_2O_3 surface, which is in accord with the previous studies [19,37]. However, the surface deformation of dehydrated surface is stronger than that for the hydrated surface, suggesting that the presence of the surface hydroxyls can improve the stability of the (110) surface.

On the other hand, in order to investigate the influence of support and surface hydroxyls on the stability of Cu_n(n = 2–4) cluster in the supported state, we have further calculated the binding energy of the Cu_n(n = 2–4) cluster supported on γ-Al_2O_3 surfaces, $E_{bind}(Cu_n/\gamma\text{-}Al_2O_3)$, which can reflect the stability of the Cu_n(n = 2–4) cluster supported on γ-Al_2O_3 surface, as listed in Table 5. We can obtain that the binding energy of Cu_n(n = 2–4) cluster in the supported state is larger than that in the corresponding isolated state, indicating the adsorption on the support stabilizes the Cu_n(n = 2–4) cluster. Meanwhile, the Cu_n cluster supported on the γ-Al_2O_3(110) surface is more stable than the corresponding cluster supported on the γ-Al_2O_3(100) surface. For the γ-Al_2O_3(110) surface, the Cu_n cluster supported on the dehydrated surface is more stable than the corresponding cluster supported on the hydrated surface, suggesting that the presence of the surface hydroxyls reduce the stability of Cu_n cluster supported on the surface.

Table 5
The binding energy of Cu_n(n = 2–4) cluster supported on γ-Al_2O_3 surfaces per metallic atom, $E_{bind}(Cu_n/\gamma\text{-}Al_2O_3)$, and the binding energy of the isolated Cu_n(n = 2–4) cluster E_{bind} (Cu_n).

n	$E_{bind}(Cu_n)$ (kJ mol^{-1})	$E_{bind}(Cu_n/\gamma\text{-}Al_2O_3)$ (kJ mol^{-1})		
	Isolated	Dehydrated (110)	Hydrated (110)	Dehydrated (100)
2	97.0	229.4 (264.9)[a]	207.8 (221.7)	175.1 (156.3)
3	104.3	220.0 (347.1)	211.2 (321.4)	183.8 (238.5)
4	113.6	216.6 (412.1)	205.5 (367.7)	186.3 (291.0)

[a]The value in parentheses are the adsorption energies of Cu_n cluster on the γ-Al_2O_3 surfaces

3.3. Growth of Cu_n cluster on γ-Al_2O_3

On the basis of above stable adsorption configuration of Cu_n(n = 1–4) cluster on the γ-Al_2O_3 surfaces, we further investigate the growth of Cu_n cluster on the γ-Al_2O_3 surfaces. To better understand the growth of Cu_n cluster, we define the growth energy for the process illustrated schematically in the Fig. 5. This energy is the energy gain (or loss) in combining an adsorbed single atom with a Cu_{n-1} cluster to form a Cu_n cluster [37]:

$$E_{grow} = E(Cu_n/\gamma\text{-}Al_2O_3) + E(\gamma\text{-}Al_2O_3) - E(Cu_{n-1}/\gamma\text{-}Al_2O_3) - E(Cu_1/\gamma\text{-}Al_2O_3)$$

With this definition, negative values of E_{grow} denote that the growth of Cu_n cluster is exothermic and thermodynamically favorable; whereas, the positive values denote that the growth of Cu_n cluster is endothermic, and thermodynamically unfavorable. The calculated growth energies on each surface together with the isolated Cu_n cluster are listed in Table 6.

As shown in Table 6, the growth of Cu_n(n = 2–4) cluster on the γ-Al_2O_3(110) surfaces are thermodynamically favorable and exothermic. On the dehydrated γ-Al_2O_3(100) surface, the growth of Cu_2 cluster is thermodynamically unfavorable, for clusters with three and four Cu atoms, the growth becomes favorable, indicating that the critical cluster size for Cu cluster growth on the dehydrated γ-Al_2O_3(100) surface is 3, and is similar to the growth of Rh cluster [37].

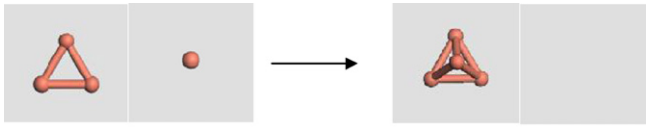

Fig. 5. Schematic illustration of the growth process considered in the definition of E_{grow}.

Table 6
Growth energy E_{grow} (kJ mol^{-1}) of Cu_n cluster supported on the γ-Al_2O_3 surfaces, and the isolated Cu_n cluster.

n	Dehydrated (110)	Hydrated (110)	Dehydrated (100)	Isolated
2	-170.5	-79.6	4.3	-193.9
3	-57.0	-50.0	-23.8	-118.9
4	-62.4	-20.3	-16.7	-141.5

The growth energy of Cu_n(n = 2–4) cluster on the γ-Al_2O_3(110) surface is smaller than the corresponding energy on the dehydrated γ-Al_2O_3(100) surface, suggesting that the growth of Cu_n(n = 2–4) cluster on the γ-Al_2O_3(110) surface is more favorable than that on the γ-Al_2O_3(100) surface. For the γ-Al_2O_3(110) surface, the growth energy of Cu_n(n = 2–4) cluster on the dehydrated surface is smaller than the corresponding energy on the hydrated surface, which indicates that the growth of Cu_n(n = 2–4) cluster is preferred on the dehydrated γ-Al_2O_3(110) surface. The presence of surface hydroxyls has a negative influence on the growth of Cu_n(n = 2–4) cluster on the hydrated γ-Al_2O_3(110) surface. More importantly, the exothermicity of Cu_n(n = 2–4) cluster supported on the γ-Al_2O_3 surfaces is smaller than those for isolated clusters, indicating that the support can reduce the growth ability of Cu_n(n = 2–4) cluster, which can inhibit the aggregations of cluster and favor the formation of small clusters.

In addition, previous studies have shown that for Pd, the growth of Pd_2 and Pd_3 clusters on dehydrated γ-Al_2O_3(100) surface are thermodynamically unfavorable [38], for the Rh cluster, Shi et al. [37] have investigated its growth on the dehydrated γ-Al_2O_3(100), hydrated γ-Al_2O_3(100) and hydrated γ-Al_2O_3(110) surfaces, and find that the Rh cluster growth is preferred on hydrated surfaces relative to the dehydrated γ-Al_2O_3 surface they examined. The above results reveal that the growth of different metals on the same γ-Al_2O_3 surfaces is also different.

4. Conclusions

In this study, density functional theory method is employed to systematically investigate the influence of surface hydroxyls on the stability and growth of Cu_n(n = 1–4) cluster on the dehydrated γ-Al_2O_3(110), hydrated γ-Al_2O_3(110) and dehydrated γ-Al_2O_3(100) surfaces. Our results show that the Cu–support interaction energy makes an important contribution to the adsorption energy of Cu_n cluster on the γ-Al_2O_3 surfaces, and Cu_n cluster deformation has a small impact on the final measured adsorption energy, and gives a negligible contribution to the adsorption energy. The adsorption of Cu_n(n = 2–4) cluster on the γ-Al_2O_3(110) surface is more stable than that on the γ-Al_2O_3(100) surface, however, for the single Cu atom, the reverse becomes true. For the γ-Al_2O_3(110) surface, the presence of surface hydroxyls has a negative influence on the adsorption of Cu_n(n = 2–4) cluster, however, it is beneficial to the stability of the γ-Al_2O_3(110) surface.

On the other hand, the growth of Cu_n cluster on the γ-Al_2O_3(110) surface is more favorable than that on the γ-Al_2O_3(100) surface. For the γ-Al_2O_3(110) surface, the presence of surface hydroxyls reduces the growth ability of Cu_n clusters, which can inhibit the aggregations and improve the dispersion of small cluster. The critical cluster size for the growth of Cu_n cluster on the dehydrated (100) surface is 3. In addition, we can find that, from a thermodynamic point of view, γ-Al_2O_3 surfaces present different trends in growth. The exothermicity of the growth for cluster on the support is smaller than that of the isolated cluster, which accounts for the property of the support to improve the dispersion of small cluster.

Acknowledgment

The work is supported financially by the National Natural Science Foundation of China (nos. 21276003, 21276171 and 20906066).

References

[1] I. Fechete, Y. Wang, J.C. Védrine, Catalysis Today 189 (2012) 2–27.
[2] A.M. Argo, J.F. Odzak, F.S. Lai, B.C. Gates, Nature 415 (2002) 623–626.
[3] H. Dropsch, M. Baerns, Applied Catalysis A: General 158 (1997) 163–183.
[4] Y. Ji, G. Liu, W. Li, W.D. Xiao, Journal of Molecular Catalysis A: Chemical 314 (2009) 63–70.
[5] G. Avgouropoulos, T. Ioannides, Ch. Papadopoulou, J. Batista, S. Hocevar, H.K. Matralis, Catalysis Today 75 (2002) 157–167.
[6] M.C. Valero, P. Raybaud, P. Sautet, Journal of Catalysis 247 (2007) 339–355.
[7] J.M.H. Lo, T. Ziegler, P.D. Clark, Journal of Physical Chemistry C 114 (2010) 10444–10454.
[8] S.Y. Wu, Y.R. Lia, J.J. Ho, H.M. Hsieh, Journal of Physical Chemistry C 113 (2009) 16181–16187.
[9] R. Grau-Crespo, N.C. Hernández, J.F. Sanz, N.H. de Leeuw, Journal of Physical Chemistry C 111 (2007) 10448–10454.
[10] P. Euzen, P. Raybaud, X. Krokidis, H. Toulhoat, J.-L. Le Loarer, J.-P. Jolivet, C. Froidefond, in: F. Schüth, K.S.W. Sing, J. Weitkamp (Eds.), Handbook of Porous Solids, vol. 3, Wiley–VCH, Weinheim, 2002, p. 1591.
[11] T. Maillet, C. Solleau, J. Barbier Jr., D. Duprez, Applied Catalysis B: Environmental 14 (1997) 85–95.
[12] F. Solymosi, Gy. Kutsán, A. Erdöhelyi, Catalysis Letters 11 (1991) 149–156.
[13] S.X. Yin, T. Swift, Q.F. Ge, Catalysis Today 165 (2011) 10–18.
[14] Y.X. Pan, C.J. Liu, Q.F. Ge, Journal of Catalysis 272 (2010) 227–234.
[15] Y.C. Chen, Z.L. Sun, L.J. Song, Q. Li, M. Xu, Physics Letters A 376 (2012) 1919–1923.
[16] N.A. Deskins, D.H. Mei, M. Dupuis, Surface Science 603 (2009) 2793–2807.
[17] G.X. Qi, J.H. Fei, X.M. Zheng, Z.Y. Hou, Reaction Kinetics and Catalysis Letters 73 (2001) 245–256.
[18] V.A. Matyshak, L.A. Berezina, O.N. Sil'chenkova, V.F. Tret'yakov, G.I. Lin, A. Ya, Rozovskii, Kinetics and Catalysis 50 (2009) 255–263.
[19] R.G. Zhang, B.J. Wang, H.Y. Liu, L.X. Ling, Journal of Physical Chemistry C 115 (2011) 19811–19818.
[20] A.M. Argo, J.F. Odzak, J.F. Goellner, F.S. Lai, F.S. Xiao, B.C. Gates, Journal of Physical Chemistry B 110 (2006) 1775–1786.
[21] B. Hvolbæk, T.V.W. Janssens, B.S. Clausen, H. Falsig, C.H. Christensen, J.K. Nøskov, Nanotoday 2 (2007) 14–18.
[22] F. Li, B.C. Gates, Journal of Physical Chemistry C 111 (2007) 262–267.
[23] R.C. Baetzold, Surface Science 36 (1973) 123–140.
[24] B.C. Gates, Journal of Molecular Catalysis A: Chemical 163 (2000) 55–65.
[25] A.M. Argo, J.F. Odzak, B.C. Gates, Journal of the American Chemical Society 125 (2003) 7107–7115.
[26] M. Montano, K. Bratlie, M. Salmeron, G.A. Somorjai, Journal of the American Chemical Society 128 (2006) 13229–13234.
[27] N.S. Babu, N. Lingaiah, R. Gopinath, P.S.S. Reddy, P.S. Sai Prasad, Journal of Physical Chemistry C 111 (2007) 6447–6453.
[28] R. Gopinath, N.S. Babu, J.V. Kumar, N. Lingaiah, P.S. Sai Prasad, Catalysis Letters 120 (2008) 312–319.
[29] D.C. Meier, D.W. Goodman, Journal of the American Chemical Society 126 (2004) 1892–1899.
[30] C.R. Henry, Surface Science Reports 31 (231-233) (1998) 235–325.
[31] M. Heemeier, M. Frank, J. Libuda, K. Wolter, H. Kuhlenbeck, M. Bäumer, H. Freund, Catalysis Letters 68 (2000) 19–24.
[32] J. Libuda, M. Frank, A. Sandell, S. Andersson, P.A. Bruhwiler, M. Bäumer, N. Martensson, H.J. Freund, Surface Science 384 (1997) 106–119.
[33] M. Digne, P. Sautet, P. Raybaud, P. Euzen, H. Toulhoat, Journal of Catalysis 226 (2004) 54–68.
[34] Y.X. Pan, C.J. Liu, T.S. Wiltowski, Q.F. Ge, Catalysis Today 147 (2009) 68–76.
[35] Y.X. Pan, C.J. Liu, Q.F. Ge, Langmuir 24 (2008) 12410–12419.
[36] D. Lomot, Z. Karpinski, Catalysis Letters 69 (2000) 133–138.
[37] X.R. Shi, D.S. Sholl, Journal of Physical Chemistry C 116 (2012) 10623–10631.
[38] M.C. Valero, P. Raybaud, P. Sautet, Physical Review B 75 (2007) 045427–45431.
[39] R.G. Zhang, H.Y. Liu, B.J. Wang, L.X. Ling, Applied Catalysis B: Environmental 126 (2012) 108–120.
[40] M. Kurtz, H. Wilmer, T. Genger, O. Hinrichsen, M. Muhler, Catalysis Letters 86 (2003) 77–80.
[41] T.W. Kim, M.W. Song, H.L. Koh, K.L. Kim, Applied Catalysis A: General 210 (2001) 35–44.
[42] F. Zaccheria, N. Ravasio, R. Psaro, A. Fusi, Chemistry-A European Journal 12 (2006) 6426–6431.
[43] B. Delley, Journal of Chemical Physics 92 (1990) 508–517.
[44] B. Delley, Journal of Chemical Physics 113 (2000) 7756–7763.
[45] J.P. Perdew, K. Burke, M. Ernzerhof, Physical Review Letters 77 (1996) 3865–3868.
[46] P. Hohenberg, W. Kohn, Physical Review B 136 (1964) B864–B871.
[47] M. Dolg, U. Wedig, H. Stoll, H. Preuss, Journal of Chemical Physics 86 (1987) 866–872.
[48] A. Bergner, M. Dolg, W. Kuechle, H. Stoll, H. Preuss, Molecular Physics 80 (1993) 1431–1441.
[49] C.H. Hu, C. Chizallet, C. Mager-Maury, M. Corral-Valero, P. Sautet, H. Toulhoat, P. Raybaud, Journal of Catalysis 274 (2010) 99–110.
[50] M.Y. Sun, A.E. Nelson, J. Adjaye, Journal of Physical Chemistry B 110 (2006) 2310–2317.
[51] H.P. Pinto, R.M. Nieminen, S.D. Elliott, Physical Review B 70 (2004) 125402–125411.
[52] J.H. Kwak, J.Z. Hu, D.H. Kim, J. Szanyi, C.H.F. Peden, Journal of Catalysis 251 (2007) 189–194.
[53] J.H. Kwak, J.Z. Hu, A. Lukaski, D.H. Kim, J. Szanyi, C.H.F. Peden, Journal of Physical Chemistry C 112 (2008) 9486–9492.
[54] C. Wolverton, K.C. Hass, Physical Review B 63 (2000) 24102–24111.

[55] G. Paglia, A.L. Rohl, C.E. Buckley, J.D. Gale, Physical Review B 71 (2005) 224115–224121.
[56] X. Krokidis, P. Raybaud, A.E. Gobichon, B. Rebours, P. Euzen, H. Toulhoat, Journal of Physical Chemistry B 105 (2001) 5121–5130.
[57] J.P. Beaufils, Y. Barbaux, Journal de Chimie Physique 78 (1981) 347–352.
[58] M. Digne, P. Sautet, P. Raybaud, P. Euzen, H. Toulhoat, Journal of Catalysis 211 (2002) 1–5.
[59] G.L. Arvizu, P. Calaminici, Journal of Chemical Physics 126 (2007) 194102–194111.
[60] G.A. Cisneros, M. Castro, D.R. Salahub, International Journal of Quantum Chemistry 75 (1999) 847–861.